

Effect of monochromatic aberrations on photorefractive patterns

Melanie C. W. Campbell, W. R. Bobier, and A. Roorda

School of Optometry, University of Waterloo, Waterloo, Ontario N2L 3G1, Canada

Received September 6, 1994; accepted September 8, 1994

Photorefractive methods have become popular in the measurement of refractive and accommodative states of infants and children owing to their photographic nature and rapid speed of measurement. As in the case of any method that measures the refractive state of the human eye, monochromatic aberrations will reduce the accuracy of the measurement. Monochromatic aberrations cannot be as easily predicted or controlled as chromatic aberrations during the measurement, and accordingly they will introduce measurement errors. This study defines this error or uncertainty by extending the existing paraxial optical analyses of coaxial and eccentric photorefractive. This new optical analysis predicts that, for the amounts of spherical aberration (SA) reported for the human eye, there will be a significant degree of measurement uncertainty introduced for all photorefractive methods. The dioptric amount of this uncertainty may exceed the maximum amount of SA present in the eye. The calculated effects on photorefractive measurement of a real eye with a mixture of spherical aberration and coma are shown to be significant. The ability, developed here, to predict photorefractive patterns corresponding to different amounts and types of monochromatic aberration may in the future lead to an extension of photorefractive methods to the dual measurement of refractive states and aberrations of individual eyes.

Key words: ocular aberrations, spherical aberration, retinal image quality, photorefractive, infant vision, vision screening.

1. INTRODUCTION

Photorefractive measures attempt to correlate photorefractive pattern width to refractive error. The purpose of this paper is to expand the existing optical theory in order better to predict the influence of monochromatic aberrations of the eye and to consider the potential of these photorefractive methods to provide a means to measure spherical and other monochromatic aberrations present in the human eye. Our analysis predicts that both the amounts of spherical aberration traditionally measured and the mixture of comatic and spherical aberrations measured in one of the authors' eyes introduce significant uncertainty into both coaxial and eccentric photorefractive measurements.

A. Photorefractive

Photorefractive methods provide rapid photographic measures of the refractive and accommodative states of infants and young children. The photographic nature and rapid speed of measurement of these methods are well suited for the limited attention and cooperation found in this age group. Three photorefractive methods have been designed: orthogonal,^{1,2} isotropic,^{2,3} and eccentric.⁴⁻⁶ In all three methods, light from a small flash source set near the aperture of a camera lens is reflected from the eye and photographed as a pattern of light whose extent varies with the refractive error and pupil size of the eye.

Orthogonal and isotropic photorefractive have similar optical designs and have been termed coaxial photorefractive because the flash source is centered along the optical axis of the camera lens. A photorefractive pattern that varies with refractive error is achieved by defocusing the camera with respect to the eye (Fig. 1). Eccentric

photorefractive is so named because the source is set eccentrically from the aperture of the camera. Unlike with coaxial methods, the camera is focused on the subject's eye. A crescent-shaped photorefractive pattern is imaged in the margin of the pupil (Fig. 1).

We previously developed a paraxial geometrical-optical analysis of these photorefractive methods that defines the extent of the photorefractive pattern at the plane of focus of the camera as a function of pupil size and refractive state.^{7,8} Predicted pattern extents can then be calculated from the recording system's measured magnification, and this does not require knowledge of the optical design of the camera lens. The geometrical analyses for coaxial and eccentric photorefractive are shown in Fig. 2. All photorefractive methods show a working range, which is a limited range over which the photorefractive pattern size changes with the eye's refractive error. This range is bordered by a dead zone, where the photorefractive pattern either is absent in the case of eccentric photorefractive or does not change in size in the case of the coaxial methods. When the refractive error becomes too large, the photorefractive pattern extent plateaus, so that increases in refraction do not produce a significant increase in pattern size. Pattern sizes in all these ranges are identified in our geometrical model.^{7,8}

B. Optics of the Eye

To date, most optical analyses of photorefractive^{2,5-8} have modeled the human eye as a single refracting surface and have been limited to a paraxial approximation. These optical models omitted the significant refractive effect caused by the chromatic and monochromatic aberrations of the eye. Recently we extended our geometrical-optical analysis of photorefractive to include the longitudinal chromatic aberration of the human eye.⁹

The magnitude of monochromatic aberrations varies among individual eyes,¹⁰ with ocular aberrations becoming increasingly important in blurring the retinal image at pupil sizes exceeding 2–3 mm in diameter.¹¹ Above a pupil diameter of 3 mm, photopic acuity falls because of the presence of aberrations.¹² One would expect, if the eye were a symmetrical optical system, that spherical aberration would be the only aberration that would blur the in-focus, axial image in monochromatic light. Positive or undercorrected spherical aberration is the type present for a single spherical surface of positive power. In this case the marginal rays intersect the optical axis nearer the refracting surface than do the paraxial rays. Negative or overcorrected spherical aberration denotes the opposite case in which the paraxial rays are refracted to a greater extent than are peripheral rays. Traditionally, spherical aberration was assumed to be the dominant aberration present in the human eye,¹¹ with evidence that either undercorrected or overcorrected spherical aberration may be found.

Spherical aberration measured in the human eye is highly variable among individuals¹⁰ but can reach magnitudes of 1.5 D at the edge of a 6-mm-diameter pupil.¹³ Variations have also been found between different meridians of a given eye¹³ and over the same pupil

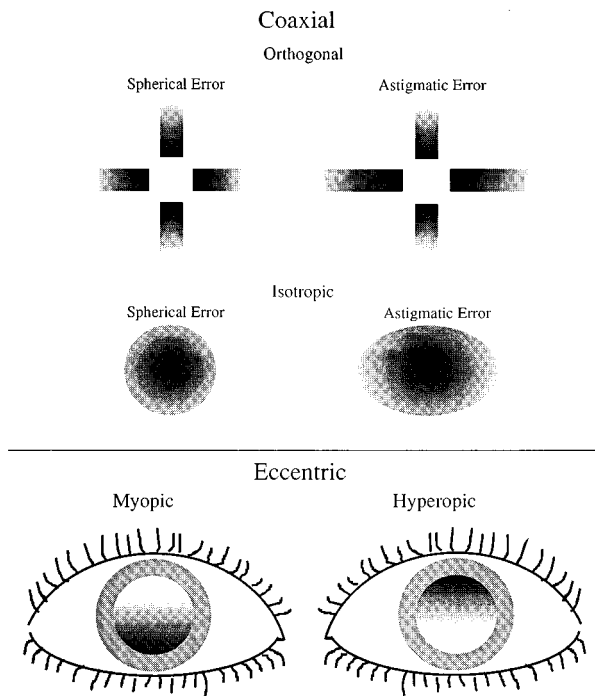


Fig. 1. Photorefractive images for orthogonal, isotropic, and eccentric photorefractive methods. For the coaxial methods (orthogonal and isotropic) the photorefractive pattern is achieved by defocusing of the light returning to the camera by a cylinder lens assembly in the former case and by defocusing the camera lens itself in the latter case. Over the working range of the instrument the length of the pattern varies in proportion to the eye's refractive error and pupil size. Eccentric photorefractive takes an in-focus picture of the pupil of the eye. Over this instrument's working range a photorefractive crescent is found in the margin of the pupil whose length varies in proportion to the eye's refractive error and pupil size. The location of the crescent is dependent on the sign of the refractive error and the circumferential position of the eccentric source. (From Bobier *et al.*⁸)

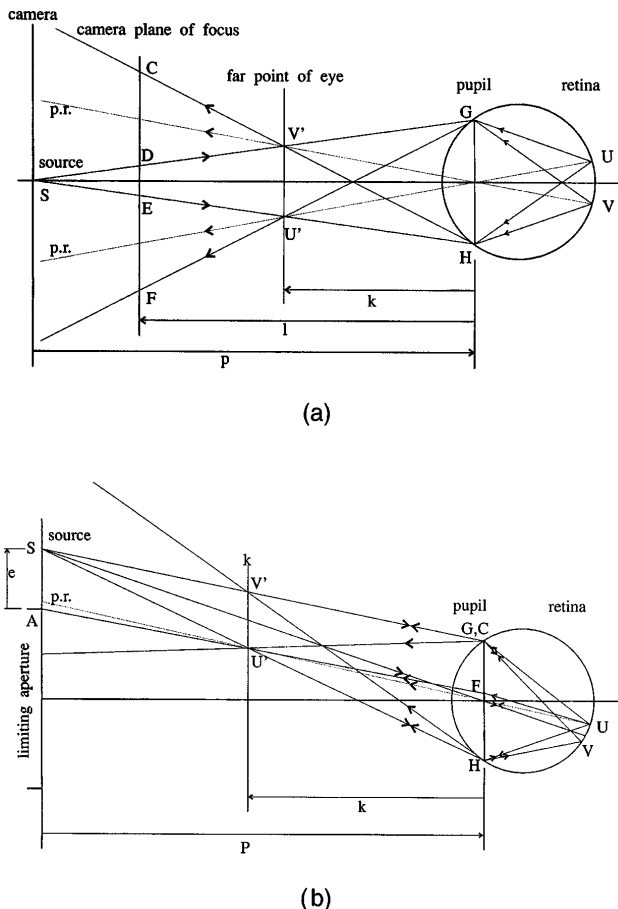


Fig. 2. (a) Coaxial photorefractive pattern for myopia in the absence of aberrations. CF denotes the photorefractive pattern size at the camera plane of focus a distance l from the eye. A refractive error within the working range of the instrument is shown for a myopic eye with the distance to the far point of the eye, k , between the eye and the camera's plane of focus ($k > l$). The flash source, S , is centered in the aperture of the camera a distance p from the pupil. Light from source S forms a retinal image, UV . An aerial image, denoted $V'U'$, conjugate to UV , is formed at the far point of the eye. The extreme rays leaving the pupil (GH) continue from $V'U'$ to the camera plane of focus and define the extreme edges of the photorefractive pattern. p.r.'s denote the principal rays passing through the pupil center. Geometrical relationships can be used to define the extent of this pattern. CD , DE , and EF can be defined by use of the similar triangles $CDV' \sim GHV'$, $EFU' \sim GHU'$, and $DES \sim GHS$. The blur diameter, CF , is given by $CF = [(2K + P)/L - 1]GH$, where K , P , and L are dioptric equivalents of k , p , and l . Similar relations have been derived for both myopic and hyperopic errors through the working ranges, dead zones, and vignetting regions.⁷ (Figure adapted from Bobier *et al.*⁷) (b) Eccentric photorefractive pattern for myopia in the absence of aberrations. CF denotes the extent of the photorefractive crescent size at the camera's plane of focus on the pupil (GH). Light source S is offset vertically a distance e from the edge of the limiting aperture A of the camera. As in the coaxial case, light from source S forms a retinal image UV . An aerial image $V'U'$ conjugate with UV is formed at the far point of the eye. The extreme ray leaving the pupil at F continues from U' to the aperture of the camera, where it represents the most extreme ray entering the camera and hence dictating the extreme edge of the photorefractive pattern. All rays emerging from between points C and F contribute to the crescent. Geometrical relationships can be used to define the extent of the pattern. Comparing the similar triangles $FHU' \sim SAU'$, one can derive the following relationship for the crescent width: $CF = GH - [eP/(-K - P)]$. Again a similar equation has been derived for hyperopic errors.⁸ (Figure adapted from Bobier *et al.*⁸)

sector between cycloplegic and natural conditions and with different degrees of accommodation.^{13,14} The presence of spherical aberration has been shown to influence the refractive state of the eye.¹⁵ More-recent measurements suggest that coma or off-axis astigmatism may have a larger effect on retinal image quality of individual eyes,^{16–18} although an average across ten eyes given by Charman shows that spherical aberration, similar to that measured classically, is the dominant average monochromatic aberration.¹⁰ Off-axis astigmatism will produce a defocus blur, the amount of which is dependent on the meridian measured. Coma, unlike spherical aberration, will produce an asymmetrical blur of a point object.¹²

Coaxial photorefractive patterns are analogous to the point-spread patterns formed in ophthalmoscopic methods of measuring the quality of the retinal image.¹⁰ Light is imaged onto the retina and then reflected back out of the eye. The image is degraded during its formation on the retina and then again during the reflection of light back out of the eye, leading to a double-pass measurement of the blur that is due to the optics of the eye. Initially, when coaxial photorefractive methods were analyzed, only the blur that is due to defocus was considered; however, the final blur is a combination of defocus and monochromatic and chromatic aberrations. The influence of chromatic aberration on the blur pattern has been calculated⁹ and is evident from the colored fringes observed in the photorefractive patterns taken with colored film.²

In eccentric photorefractive the source is offset from the edge of the camera aperture. Colored fringes that are due to the chromatic aberration of the eye are also observed in this method,⁴ and their expected extent has been calculated.¹⁹ Eccentric photorefractor designs can be similar to the Foucault knife-edge method^{6,20,21} used by Berny and Slansky²² to analyze the monochromatic aberrations of the eye. At that time, analysis of the results of one eye took several months. Recently work has been initiated to examine the effect of the eye's comatic aberration on the eccentric photorefractive pattern by using a point source.²³ Others²⁴ have shown that spherical aberration will affect a knife-edge pattern differently for myopic and hyperopic defocus. The theoretical equations for the irradiance patterns expected in a linear knife-edge photoscreener in response to specific aberration types and sample images have been simulated.²¹ However, the study presented here will be the first, to the authors' knowledge, to explore the changes in size of the photorefractive pattern associated with the amounts and types of aberration expected in the human eye and the resulting uncertainty introduced in the measurement of the eye's refractive error.

In this study we extend the previously derived paraxial equations for describing the extents of coaxial and eccentric photorefractive patterns; we examine how monochromatic aberrations will affect the refractive properties of the human eye and how they will in turn affect the photorefractive patterns and the uncertainty of photorefractive measures. We explore the possibility that, in conjunction with recent computing technology, the application of video photorefractive techniques could, with slight modifications, be extended to provide rapid mea-

asures of the aberrations of the eye in addition to measures of refractive and accommodative states.

2. OPTICAL ANALYSIS OF PHOTOREFRACTION OF THE HUMAN EYE

Initially we review the paraxial geometrical optical analysis previously derived.^{7,8} This analysis is then extended to the simplest case of spherical aberration in combination with a particular sign of refractive error in coaxial photorefractive. This extended analysis will be shown to be analogous to equations derived previously to describe the effects of chromatic aberration.⁹ A more general analysis of the effect of monochromatic aberrations will then be derived. Both eccentric and coaxial photorefractive will be considered.

A. Paraxial Optical Analysis

1. Coaxial Photorefractive

The paraxial optical theory for coaxial photorefractive is shown in Fig. 2(a) for a myopic eye. Rays from source S form a retinal stimulus pattern (*UV*), which is then diffusely reflected by the eye to form an aerial image at the far point plane of the eye. The projection of this image onto the plane of focus of the camera (*CF*) defines the extent of the photorefractive pattern. The entering and exiting rays at the extreme edges of the pupil (*GH*) define the extreme edge of the retinal image and the photorefractive pattern. The case is similar for longitudinal chromatic aberration, but the analysis must be repeated for two far-point positions representing the extreme blue and red ends of the visible spectrum.⁹

2. Eccentric Photorefractive

The paraxial model for eccentric photorefractive is shown in Fig. 2(b). As in the coaxial method, a retinal image (*UV*) of eccentric source S is diffusely reflected to form an aerial image at the far point of the eye. The projection of the aerial image onto the camera's plane of focus at the pupil defines the size of the photorefractive pattern. The ray entering the extreme edge of the pupil, H, forms the extreme edge of the retinal blur, and the ray exiting from the edge of the blur through F, the far point U', and the edge of the camera aperture, A, forms the edge of the photorefractive crescent. As for coaxial photorefractive, we have shown that the effect of longitudinal chromatic aberration can be predicted by repetition of this paraxial analysis for two far points, which represent the extreme blue and red ends of the source spectrum.^{9,19}

B. General Optical Analysis

If a perfect optical system is described geometrically, all rays from a point object come to focus at a point image. The far point of the eye is at a distance k_0 from the eye, the distance at which a point source must be placed to be conjugate with the retina. If the optical system is imperfect because of the presence of monochromatic aberrations, all rays from a point source will not focus to a single image point. Figures 3 and 4(a) show an example of one such aberration, spherical aberration. The power of the eye will vary with the position \mathbf{r} of entry of a light ray in the entrance pupil of the eye. Thus the far-point distance $k(\mathbf{r})$ from which a ray is focused on the retina

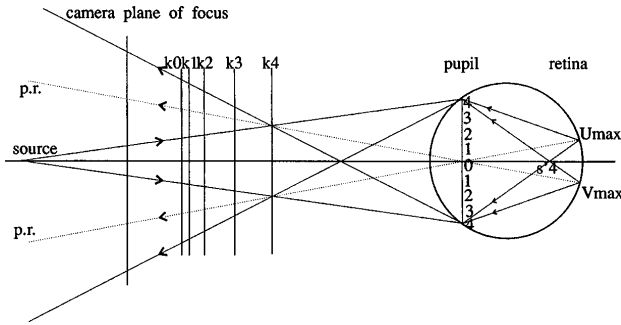


Fig. 3. Coaxial photorefraction for a myope with undercorrected spherical aberration. The paraxial far point (k_0) and the far points corresponding to increasingly more marginal rays (k_1 – k_4) are shifted monotonically from the camera plane of focus toward the eye. In this special case the photorefractive pattern extent is determined by the rays entering and leaving the extreme edges of the pupil. The geometry is the same as for the paraxial case [Fig. 2(a)], except that the far point is varying with the position of the ray entering the pupil. The returning rays, determining the pattern extent, pass through the far point corresponding to rays at the margin of the pupil. As a result, the photorefractive pattern increases in size. The size of the blur in this case can be calculated by insertion of the marginal far-point value into the equation in the caption to Fig. 1.

is a function of the position \mathbf{r} of entry of the ray being considered. A ray from the far point, a distance $k(\mathbf{r})$ from the eye, measured along a principal ray incident upon the pupil at a position \mathbf{r} , will intersect the principal ray at the retina. Optical paths are reversible, so rays reflected from a point on the retina at a position \mathbf{r} in the pupil will intersect the principal ray from that point a distance $k(\mathbf{r})$ from the eye, measured along the principal ray.

In our analysis we use the function $k(\mathbf{r})$ to represent the aberrations in the eye. If there are no aberrations present in the eye, $k(\mathbf{r})$ will be constant and equal to the paraxial far-point distance k_0 . If only spherical aberration is present, $k(\mathbf{r})$ is dependent only on the radius of the entering ray and \mathbf{r} is represented as the scalar r . We will restrict our analysis to measurements along the principal astigmatic axes. Along these axes the crescent extents are due only to variations in power along the meridian that joins the source to the center of the pupil. Along other axes the dependence is more complex.²⁵

C. Assumptions

The following assumptions will be made in the general optical analysis:

- (i) Diffraction effects are negligible.

A geometrical theory is used that ignores diffraction effects. This assumption is valid in regions where the aberrations or defocus are greater than 1λ .

- (ii) The light source is simulated as a single point.

This is a valid assumption because the least eccentric point of the source determines the maximum extent of the crescent.

- (iii) The size of the blur on the retina is aplanatic.

In the working ranges chosen, we assume that the blur on the retina is sufficiently small that the aberrations will be the same for all points on the retinal blur that act as secondary point sources.

- (iv) $k(\mathbf{r})$ will define the aberration of the point light source.

The aberrations are dependent on the optical system that is being measured as well as on the distance of the source from the system. Light reflected out of the eye will suffer from aberrations defined by $k(\mathbf{r})$. However, the retinal image will suffer from aberrations that are dependent on the distance of the photorefractive source from the eye relative to the paraxial refractive state. We will assume that the light source is a sufficient distance from the eye and that the aberrations vary slowly enough with the vergence of the incident light that the function $k(\mathbf{r})$ also defines the aberration of the retinal image.

- (v) We assume that the angles are small.

The far-point distance from the eye that corresponds to each point on the retina will always be measured along the optical axis of the system. For retinal blurs subtending small angles this is a reasonable approximation, as the actual distance varies with the cosine of the angle between the principal ray and the optical axis.

- (vi) The retina is modeled as a perfect diffuse reflector.

(vii) The entrance pupil and the first principal plane of the eye are assumed to be coincident so that $k(\mathbf{r})$ can be measured.

The theory does not explicitly consider rays that enter the eye. This allows us to use a more generalized model of the eye. For clarity, however, the figures use a reduced eye with a single refracting surface.

- (viii) The camera aperture is sufficiently large to capture all the rays that enter beyond the limiting aperture.

D. Coaxial Photorefraction: Optical Analysis in the Presence of Spherical Aberration

For coaxial photorefractive methods, for certain cases of spherical aberration, we can use an analysis similar to that used for chromatic aberration. These cases are those in which the sign of the spherical aberration is positive (undercorrected) and the refractive error of the eye is negative (myopic with respect to the camera plane of focus) and those in which the spherical aberration is negative (overcorrected) and the refractive error is positive (hyperopic with respect to the camera plane of focus). In both cases the paraxial far point and the far points that correspond to increasingly more marginal rays are shifted monotonically from the camera plane of focus. The former situation is shown in Fig. 3. The photorefractive pattern edge will be determined by the rays that are exiting from the pupil margins, and the equations that define the pattern extent are analogous to those derived for chromatic aberration⁹:

$$CF = \left\{ \frac{2K_y + P}{L} - 1 \right\} GH, \quad (1)$$

where CF is the extent of the photorefractive pattern, K_y is the refractive state corresponding to rays through the pupil margin, L is the dioptric equivalent of the camera-plane-of-focus distance from the eye (l), P is the dioptric equivalent of the camera and source distance from the eye (p), and GH is the pupil diameter.

E. Coaxial Photorefraction: Optical Analysis for More-General Monochromatic Aberrations

The optical analysis is more complex for other combinations of spherical aberration and defocus error, i.e., when

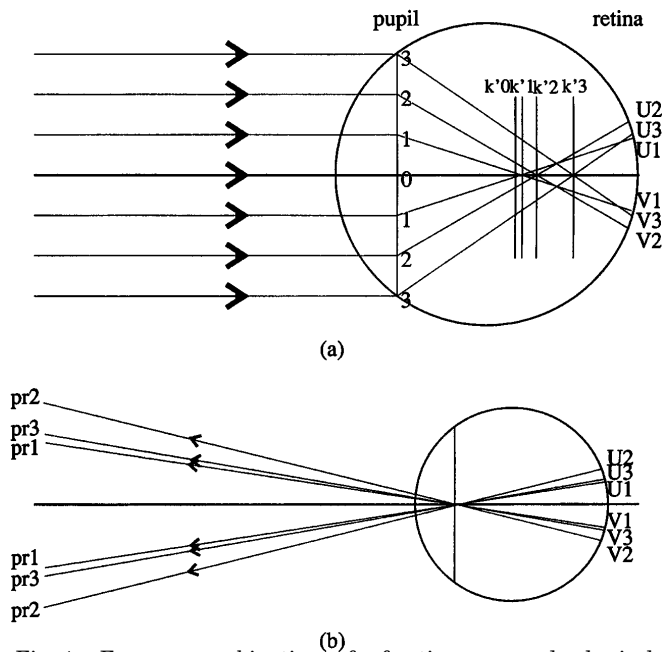


Fig. 4. For some combinations of refractive error and spherical aberration the maximum blur spot diameter on the retina is not necessarily defined by the beam entering the margin of the pupil, as illustrated here for a myope with overcorrected spherical aberration. (a) Enlarged view of what takes place in the eye with respect to the focus as a function of the radius. The focal points for the different entering radii are denoted k'_i . In this example the maximum spot size is determined by the ray entering pupil position 2. (b) The most divergent principal ray emerges from the maximum extent of the blur on the retina, U_2 . Therefore, when the most divergent ray is found, the maximum extent of the blur on the retina has also been found. p.r._i are the principal rays originating at points U_i on the retina.

the refractive error is myopic and the spherical aberration is negative or when the refractive error is hyperopic and the spherical aberration is positive. The optical analysis will also be more complex when other monochromatic aberrations such as coma are present. For these cases, if the magnitude of the aberrations is sufficient, then the rays entering the pupil margin do not define the extreme edge of the blur circle on the retina [Fig. 4(a)], nor do the rays leaving the extreme edge of the pupil form the extreme edge of the photorefractive pattern. Furthermore, the critical entering rays that form the edge of the retinal blur and the exiting rays that form the edge of the photorefractive pattern do not necessarily intersect the pupil at the same position (Fig. 5). As the refractive error increases, rays from the pupil margin are more likely to define the extent of the photorefractive pattern. Therefore a double-pass optical analysis must be considered.

In the most general case, the first step is to define the position in the pupil of the entering ray that defines the maximum spot size on the retina. This point is illustrated in Fig. 4(a) for a myopic eye with negative spherical aberration. It follows [Fig. 4(b)] that the principal rays leaving through the center of the pupil that intersect the camera plane farthest from the optical axis emerge from the edges of the blur on the retina, so that the most divergent principal ray originates from the extreme edge of the retinal blur. One ray from this retinal point will then define the edge of the photorefractive pattern (Fig. 5).

One can find geometrically the edge of the blur on the retina that will give rise to the most divergent principal ray by constructing principal rays passing through the center of the pupil [Fig. 6(a)], yielding the result that the intersection distance from the optical axis of a principal ray at the source plane is $x(\mathbf{r})$, where

$$x(\mathbf{r}) = \mathbf{r} \cdot \frac{[p + k(\mathbf{r})]}{-k(\mathbf{r})}, \tag{2}$$

p is the distance from the source to the entrance pupil of the eye, and $k(\mathbf{r})$ is the distance to the far point from the eye for a ray entering the pupil at position \mathbf{r} and intersecting the retina at $\mathbf{U}(\mathbf{r})$. The variable \mathbf{r} is the vector distance from the optical axis at which the ray enters the pupil. The formula is in terms of the far-point distance of the eye, $k(\mathbf{r})$, whose variation with \mathbf{r} is a measure of the degree of aberration present in the eye. In the absence of aberrations $k(\mathbf{r})$ is constant, and the principal ray from the edge of the retinal blur then intersects the source plane at a distance x_{\max} from the axis such that

$$x_{\max} = r \frac{[p + k]}{-k}, \tag{3}$$

where r is the scalar distance in the pupil measured from the optical axis. In either the presence or the absence of aberrations, maximizing Eq. (2) with respect to \mathbf{r} yields the entering radius of the ray that defines the extreme edge, U_{\max} , of the blur on the retina. The principal ray reflected from U_{\max} through the pupil center will intersect the source plane at the maximum value of x , x_{\max} . The position U_{\max} and value x_{\max} will be influenced both by the defocus of the eye from the source plane and by the aberrations present.

The second step in the method is to find the ray that defines the maximum photorefractive pattern extent. This will be a ray originating from U_{\max} . The rays originating from point U_{\max} on the retina and exiting from the eye

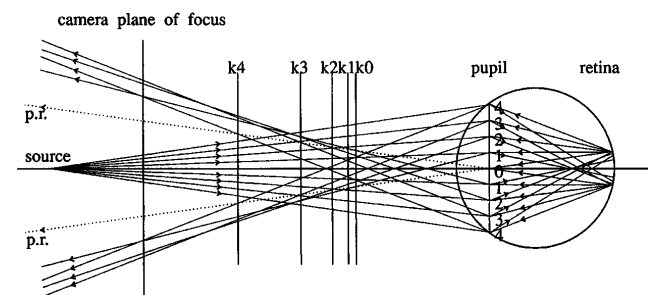


Fig. 5. This ray diagram demonstrates that in most cases, for spherical aberration, when the far points do not increase monotonically from the camera plane of focus, more in-depth analysis is required for coaxial photorefractive. It can be seen that the marginal ray does not define the maximum blur spot on the retina or the maximum pattern extent at the camera plane of focus. It can also be seen that the maximum pattern extent is dependent on the plane of focus of the camera. In this case the maximum pattern extent is determined by the rays leaving the pupil at the points labeled 3. If the plane of focus were positioned slightly closer to the eye, the maximum would be defined by a different exiting ray. The method of determining the maximum pattern extent is detailed in Figs. 6 and 7. All outgoing rays drawn originate from points U_{\max} and V_{\max} at the edge of the retinal blur.

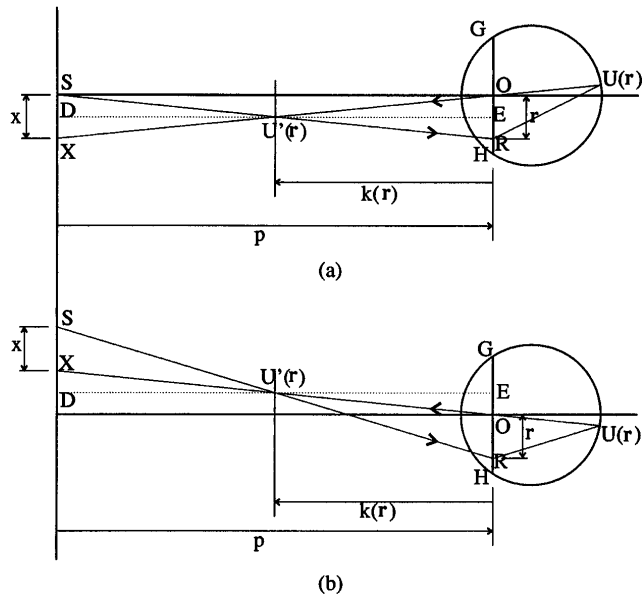


Fig. 6. This figure defines the principal ray corresponding to the edges of the image: (a) and (b) are ray traces used to find the intersection of the principal ray from the edges of the image with the camera plane for coaxial and eccentric methods, respectively. The distance of the intersection of the principal ray, x_i , is measured from the source S, so the treatment for both methods is the same. As the radius of entry r of ray SR varies, the intersection point of the principal ray OX also varies. Ray OX goes through $U'(r)$ conjugate with the position of the blur on the retina, $U(r)$, where $U(r)$ varies with the radius r of the entering ray. The distance x can be defined by the use of the similar triangles, $SXU'(r) \sim ORU'(r)$ and $XDU'(r) \sim OEU'(r)$. Finding the most divergent principal ray requires maximizing the resulting equation [Eq. (2) in the text] with respect to the entering radius r . (DE is a construction.)

will also be influenced by aberrations and defocus and will not intersect the principal ray at a single point. Figure 7 demonstrates how geometrical optics are used to define the pattern extent as a function of the radial position r in the pupil of the ray exiting from the extreme edge of the blur on the retina. The pattern extent is defined at the plane of focus of the camera. The principal ray intersects the camera's plane of focus at a distance from the optical axis:

$$AB = -x_{\max} \frac{l}{p} \tag{4}$$

Rays return from U_{\max} through points R in the pupil and intersect the camera plane of focus at C. The distance BC for a given position r in the pupil is determined from similar triangles. The radius of the pattern extent is then given by $AB + BC$ or

$$CA(r) = -x_{\max} \frac{l}{p} + r \cdot \frac{[-l + k(r)]}{-k(r)} \tag{5}$$

In the absence of aberrations, $k(r)$ is a constant and the maximum value of CA is given for r equal to the pupil radius, and Eq. (5) reduces to Eq. (1) with K_y now equal to the constant refractive state across the whole pupil. In the presence of aberrations one finds the maximum pattern extent numerically by finding the maximum value of Eq. (5) for r between zero and the maximum pupil diameter. The maximum value of CA may be different in different meridians in the presence of coma or off-axis astigmatism.

F. Eccentric Photorefractive: Optical Analysis for General Monochromatic Aberrations

In eccentric photorefractive there is no case for which the geometrical analysis is analogous to that used for chromatic aberration.⁹ The first step of the general method is similar to that used for coaxial photorefractive and finds the maximum pattern extent on the retina. The distance, x , to the intersection of the principal ray with the source plane measured from the source is shown in Fig. 6(b). In eccentric photorefractive, the source is not on the optical axis of the eye [Fig. 6(b)]. Equation (2) can, however, still be used to define the distance x for a principal ray reflected from a point $U(r)$ on the retina. r is the radial position of entry in the pupil of the ray that formed $U(r)$. Equation (2) is then maximized with respect to the radius r to yield the most divergent principal ray reflected from the edge, U_{\max} , of the blur on the retina (Fig. 8).

The second step is to find the returning ray that defines the edge of the photorefractive pattern, in this case the crescent that will appear in the pupil. In Fig. 8 the ray of interest exits from the pupil at position F. It is necessary to find the ray returning from U_{\max} that intersects the limiting aperture A of the camera. Figure 8 shows the formation of U_{\max} by incoming rays and the rays reflected back from U_{\max} . Rays from U_{\max} intersect the principal ray at positions $k(r)$ determined by the monochromatic aberrations present.

Using geometrical optics, from Fig. 9 we derived an equation that determines the intersection point on the

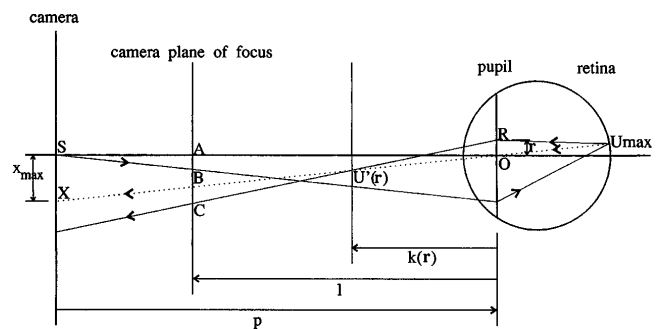


Fig. 7. Maximum photorefractive pattern extent for coaxial photorefractive. This diagram is a ray trace of the rays leaving the pupil. Point U_{\max} on the retina represents the most extreme edge of the spot on the retina found by maximizing the distance SX in Fig. 6. The ray emerging from U_{\max} , which passes through the center of the pupil (dotted curve), is the most divergent principal ray found previously. Rays reflected from point U_{\max} will intersect the principal ray at far points determined by the type of monochromatic aberration and the exit radius r of these rays in the pupil. The figure shows only one such ray, leaving the pupil at R, striking the source plane at X, and intersecting the principal ray at $U'(r)$ a distance $k(r)$ from the eye. The objective is to define the extent, AC , of the photorefracted pattern from the eye at the camera plane of focus as a function of the radius r where the ray leaves the pupil. x_{\max} represents the distance at which the most divergent principal ray intersects the source plane. This ray intersects the camera plane of focus at B, a distance $(x^*l)/p$ from the optical axis. The distance BC within which returning rays intersect the camera plane of focus can be determined by the use of the similar triangles, $BCU'(r) \sim ORU'(r)$, where $U'(r)$ is the far point corresponding to a ray originating at the edge of the image and leaving the pupil at position r . The resulting equation [Eq. (5) in the text] must be maximized with respect to the exiting radius to yield the maximum blur diameter.

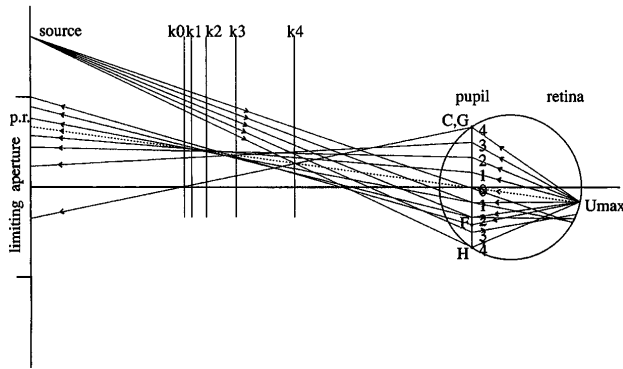


Fig. 8. Maximum photorefractive pattern extent for eccentric photorefraction. This example is a ray trace for a myopic eye with positive spherical aberration. In this case the marginal entering ray defines the most extreme edge of the blur on the retina. Each returning ray (from U_{max}), through position i in the pupil, intersects the principal ray at the corresponding far point, k_i . The returning ray that defines the crescent width is the ray that intersects the limiting aperture of the camera lens. In the example this ray emerges from point F on the pupil. Rays from C to F define the crescent that will appear in the pupil. A detailed analysis is given in the following figures.

camera plane of a ray returning from U_{max} . The separation of the intersection point, $Y(\mathbf{r})$, from source S is $y(\mathbf{r})$ equal to the sum of x_{max} and $z(\mathbf{r})$:

$$y(\mathbf{r}) = x_{max} + \mathbf{r} \cdot \frac{[p + k(\mathbf{r})]}{-k(\mathbf{r})} \quad (6)$$

The ray reflected from U_{max} that will intersect the source plane at the limiting aperture of the camera, A in Fig. 9, is the one leaving the pupil at a radius for which $y(\mathbf{r}) = e$, where e is the distance of the camera aperture from the source. This ray forms the edge of the crescent recorded in the pupil. The complete crescent in the case of Fig. 8, extending from the top edge of the pupil to the ray through F , intersecting the edge of the aperture, is formed by rays from all points on the retina reflected through the pupil between C and F with vergences allowing them to be captured by the camera aperture.

The methods illustrated and the equations derived apply to the case of the myopic eye. The theory can easily be extended to the hyperopic case and also for the dead-zone regions (see Appendix A). Some care, however, must be taken with the sign conventions.

G. Numerical Analysis of the Effect of Aberrations on Photorefractive Pattern Extents

If only third-order spherical aberration were present in the eye, as has been shown on average,¹¹ then²⁶

$$k(r) = k_0 + cr^2, \quad (7)$$

where r is the scalar distance from the optical axis, $k(r)$ is the distance to the far point, k_0 is the paraxial far-point distance, and c is a constant that varies with the amount of spherical aberration present. For negative or overcorrected spherical aberration, $c > 0$ and $K_y - K_0 > 0$, where K_0 and K_y are the refractive errors that correspond to the paraxial and marginal rays, respectively. For undercorrected or positive spherical aberration, $c < 0$ and $K_y - K_0 < 0$.

A computer program was used to simulate the effects

of spherical aberration for both eccentric and coaxial photorefraction. Spherical aberration varies from subject to subject and may be a combination of third and fifth orders.¹⁰ Over a 6-mm-diameter pupil values of spherical aberration up to 1.5 D have been measured.¹³ For the first simulation, spherical aberration was assumed to be third order and is described by Eq. (7). Values of the constant in Eq. (7) corresponding to spherical aberration of 1.5 D overcorrected and 1.5 D undercorrected at the edge of an 8-mm pupil were calculated. Equations (2) and (4)–(6) were evaluated numerically on the computer, and the maximum pattern extent was derived for rays leaving the source and reflected from the retina through pupil positions between 0 and 8 mm at 0.1-mm intervals. The analysis was performed for both coaxial and eccentric photorefraction. As no information is available on the likely variation of monochromatic aberrations with refractive error, the same amount of aberration in dioptric terms at the edge of the pupil was simulated for a complete range of refractive errors.

The results of the simulation for coaxial photorefraction for a myopic camera defocus are shown in Fig. 10(a). Depending on the signs of the refractive error and the spherical aberration, the pattern extent may be increased or reduced from that expected in the absence of aberration. The extent of the dead zone and the size of patterns in the dead zone may also be affected. Outside the dead zone the constant amount of aberration in dioptric terms produces an almost constant increase or decrease in the pattern extent. If aberrations of this order were present but a paraxial analysis were applied, errors in the estimated central refractive error of up to ± 1.5 D would occur throughout the working range.

The results of the simulation for eccentric photorefraction for a camera distance of 1 m and a source eccentricity

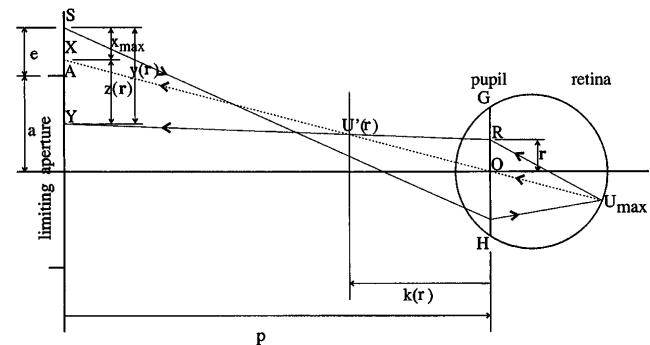


Fig. 9. Maximum crescent width for eccentric photorefraction. This diagram is a ray trace of the rays leaving the pupil. Point U_{max} on the retina represents the most extreme edge of the blur on the retina, and the ray emerging from it that passes through the center of the pupil (dotted line) is the most divergent principal ray, which was found in Fig. 6(b). Rays reflected from point U_{max} will intersect the principal ray at far points $U'(\mathbf{r})$ determined by the type of monochromatic aberration and their position \mathbf{r} of exit in the entrance pupil. The objective is to define the point where the returning rays intersect the source plane. The ray that intersects the source plane at the limiting aperture defines the crescent width. The point where the principal ray intersects the source plane is at a distance x_{max} from the source. The returning rays intersect at a distance $z(\mathbf{r})$ from this point. This distance can be determined by use of the similar triangles $XYU'(\mathbf{r}) \sim ORU'(\mathbf{r})$. The position of the intersection of the ray from the source is given by $y = x + z$. The crescent width is then defined by the radius r for which $y = e$, the eccentricity.

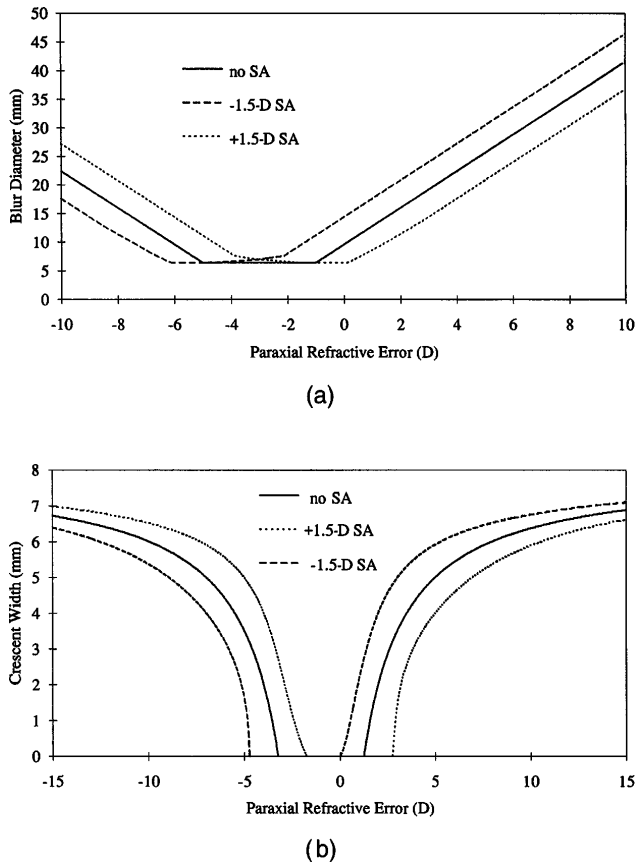


Fig. 10. Results for a numerical calculation performed with two opposite signs of spherical aberration (SA) of 1.5 D for (a) coaxial and (b) eccentric photorefraction. (a) For coaxial photorefraction a camera distance of 1 m, a camera defocus of 0.2 m in front of the subject, and a pupil size of 8 mm were assumed. We find that there is a linear shift in the pattern extent in the direction of the SA. This is because the rays that are defining the maximum pattern extent generally exit at the margin of the pupil. The SA also affects the dead-zone region. The refractive error estimate will generally be off by the amount of aberration at the margin of the pupil. (b) For eccentric photorefraction the source eccentricity was 18 mm, the pupil size was 8 mm, and the camera distance was 1 m. The shift in pattern extent with SA is not linear but varies with the crescent width. In eccentric photorefraction, 1.5 D SA can affect the uncertainty in the refractive error estimate by amounts well above this.

of 18 mm are shown in Fig. 10(b). Again, depending on the sign of the refractive error and the spherical aberration, the pattern extent may be increased or reduced from that expected in the absence of aberration. The effect is largest at intermediate and high refractive errors and less at low refractive errors. If aberrations of this order were present but a paraxial analysis were applied, at refractive errors of ± 1 or ± 3.5 D, errors in the estimated central refractive error of approximately ± 1.3 D would occur. At ± 10 D, errors of ± 3 D would occur. This is consistent with the greater measurement errors generally encountered in the asymptotic region of the function.⁴

To simulate the actual effects of aberrations in an eye, the aberrations of the left eye of one of the authors (subject MC), measured at a 2-m distance in the horizontal meridian for a dilated pupil, were fitted with the use of a method previously described,²⁷ as a function of pupil position. The blur measured varied as a function of pupil

position in the following manner:

$$\text{Blur}(r) = b_1(r - r_0)^2 + c_1(r - r_0)^3 + b_2(r - r_0)^4, \quad (8)$$

where r_0 , b_1 , b_2 , and c_1 are constants; r_0 is the position of the axis of symmetry of the aberrations; b_1 and b_2 are the coefficients of coma, which in this eye have opposite signs; and c_1 is the coefficient of spherical aberration.

We then converted the measured blur into values of dioptric refractive error, K , using the following equation:

$$K(r) = \frac{\text{blur}(r)}{(rl)}, \quad (9a)$$

where l is the distance at which the aberrations were measured.

Or, in this eye,

$$K(r) = B_1(r - r_0) + C_1(r - r_0)^2 + B_2(r - r_0)^3, \quad (9b)$$

where the terms in B_1 and B_2 represent coma and the term in C_1 represents spherical aberration that is symmetrical about an axis displaced r_0 from the pupil center. For subject MC, $B_1 = 0.2849$, $C_1 = 0.0518$, $B_2 = -0.0243$, and $r_0 = -1.14$ mm.

Equations (2), (4), and (5) were maximized to give the coaxial photorefraction pattern extent. Because of the asymmetry of $K(r)$ the ray intersections had to be calculated independently for all rays along the meridian, entering and exiting on both sides of the axis of symmetry. To generate a plot of pattern extent versus refractive error (Fig. 11), we simulated artificial refractive errors as if refractive error were being induced by aberration-free lenses and the aberrations of the eye-lens system were unchanged in dioptric terms as a function of refractive error. From Fig. 11 it can be seen that, for the aberrations present in this eye, the pattern extent measured in the horizontal meridian will be increased by an amount equivalent to an error in the working range of up to 1.5 D above the actual paraxial refractive state.

3. DISCUSSION

The following points can be summarized from this analysis: spherical and other monochromatic aberrations can change the predicted photorefraction pattern extent for both coaxial and eccentric methods. Although we have shown^{9,19} that chromatic aberration will also change the photorefraction pattern, this change is always such that the pattern is increased and the effect is consistent between individuals given that measurements of longitudinal chromatic aberration in adult subjects show standard deviations of 0.20 D or less.²⁸⁻³⁰ However, spherical and other monochromatic aberrations will either decrease or increase the pattern, depending on the sign of the aberrations and the sign of the eye's refractive state. For example, we have shown that the possible presence on average of spherical aberration will produce a large uncertainty in the refractive state measured that can exceed the maximum dioptric amount found.

The analysis of real aberrations within one eye predicts a substantial shift in measured refractive error for this subject. Additionally, the measurement uncertainty that is due to longitudinal chromatic aberration can be

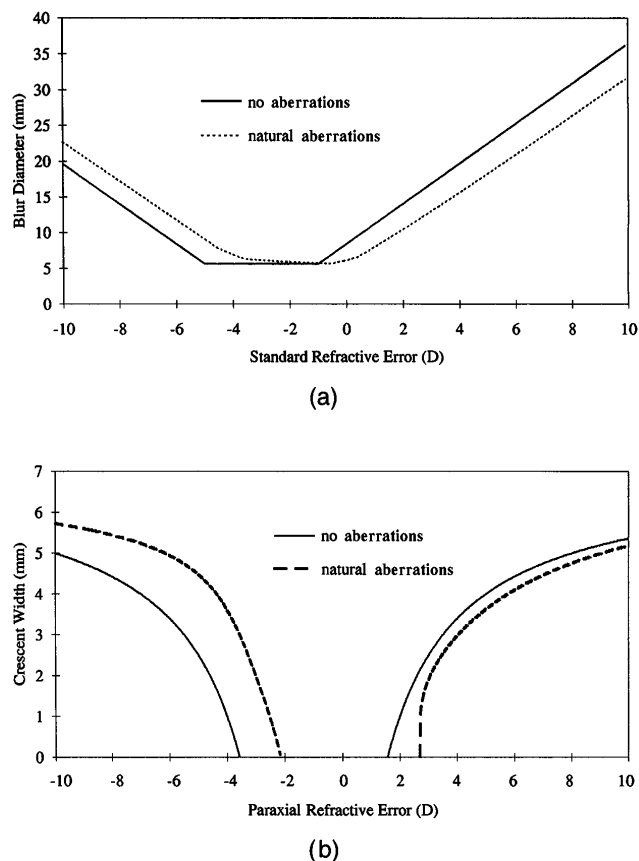


Fig. 11. (a) Coaxial and (b) eccentric photorefractive pattern extents expected for a perfect eye compared with that expected for a real eye. The aberrations across the horizontal meridian of the eye of one of the authors (subject MC) have been measured and consist of both spherical aberration and comatic-type aberrations. The coaxial and eccentric equations were solved given the measured variation of the far point with pupil position $k(\mathbf{r})$. Because of the asymmetry of the aberrations, the pattern extent was calculated for rays entering the pupil on either side of the center of the pupil. The total expected pattern extent in the horizontal as a function of artificially induced refractive error is shown. A pupil size of 7 mm and a camera distance of 1 mm were simulated. For (a) the camera defocus was 0.2 m in front of the eye. For (b) the eccentricity used was 18 mm.

reduced when colored film is used and a correction is made for blue- and red-colored crescents,⁴ whereas the variability of monochromatic aberrations among subjects precludes an analogous correction. Generally, one calibrates photorefractive investigations of infants and children by photographing induced refractive changes in the eyes of older adult subjects.^{4,31} This calibration is often performed with trial ophthalmic lenses in front of the eye. First, in the adult eye, the relationship, if any, between refractive error and the presence of aberrations is not well understood. Second, amounts of chromatic and monochromatic aberrations in the developing eye are not well studied. In the case of longitudinal chromatic aberration the difference between the adult and the infant eye can to some degree be calculated based on the increased dioptric power of the infant eye.³² However, monochromatic aberrations cannot be approximated in this way. What empirical evidence there is from retinoscopic measures of young children under 6 years of age³³ suggests that the predominant direction of spherical aberration changes with development from negative to positive. Thus the

eyes for which photorefractive is calibrated may have significantly different amounts and signs of monochromatic aberrations from those eyes being tested.

It should be noted that all objective methods that refract the eye, such as retinoscopy³⁴ and autorefractors, are affected by monochromatic aberrations. The magnitude of this effect will be related to the degree to which peripheral rays affect the measurement. We have shown that the present analysis of photorefractive methods is highly susceptible to spherical aberrations, given that over much of the range of refractive errors extreme rays from the pupil will dictate the position of the edge of the pattern. Retinoscopy would in theory be less susceptible in that it can be modeled to consider only the light returning from the central 3 mm of the pupil.

Recently we initiated studies that provide empirical measures of the effect of varying amounts and direction of spherical aberration on the photorefractive pattern. Although the overall size of the patterns can be found to change in accordance with our theory, we believe that identifying changes in the relative intensity of the light distributed across the pattern caused by monochromatic aberrations, in addition to the overall extent of the pattern, may prove to be an important means of analysis.

If this analysis were extended to describe the effects of monochromatic aberrations on the intensity distributions in photorefractive patterns, it might also lead to a modification of photorefractive methods to measure monochromatic aberrations as well as refractive state. Intensity distributions in coaxial photorefractive will be affected by diffraction of the returning light about the flash source. Thus eccentric photorefractive used with a source at a small eccentricity appears the more likely candidate for the measurement of monochromatic aberrations. The ideal parameters of such a system remain to be determined.

APPENDIX A

Coaxial Photorefractive Equations and Sign Conventions

For the principal rays:

$$x(\mathbf{r}) = \mathbf{r} \cdot \frac{[p + k(\mathbf{r})]}{-k(\mathbf{r})};$$

p is positive,
 $k(\mathbf{r})$ is negative for myopia and positive for hyperopia,
 $x(\mathbf{r})$ is positive for rays above the source and negative for rays below the source,
 \mathbf{r} is positive for rays above center and negative for rays below center (i.e., up is positive and down is negative).

For maximizing the returning rays:

$$CA(\mathbf{r}) = -x_{\max} \frac{l}{p} + \mathbf{r} \cdot \frac{[-l + k(\mathbf{r})]}{-k(\mathbf{r})};$$

up is positive and down is negative,
 l is negative in front of the eye and positive when light is focused behind the eye.

Eccentric Photorefractive Equations and Sign Conventions

For the principal ray:

$$x(\mathbf{r}) = \mathbf{r} \cdot \frac{[p + k(\mathbf{r})]}{-k(\mathbf{r})} \quad (\text{same as for coaxial}).$$

For the rays that define the crescent:

$$y(\mathbf{r}) = x_{\max} + \mathbf{r} \cdot \frac{[p + k(\mathbf{r})]}{-k(\mathbf{r})};$$

$y(\mathbf{r})$ is positive for rays above the principal ray and negative for rays below the principal ray.

A crescent edge is observed when $y(\mathbf{r}) = e$, the eccentricity. In the program a negative value for e represents an eccentricity below the source and a positive value represents an eccentricity above the source. The \mathbf{r} value for which $y(\mathbf{r}) = e$ may be positive or negative. A positive value represents a position above and a negative value represents a position below the geometrical center of the pupil.

ACKNOWLEDGMENTS

The assistance of Linda Voisin in the preparation of this manuscript is gratefully acknowledged. This work was supported by Natural Sciences and Engineering Research Council (NSERC) Canada Research Grants and Strategic Grant to W. R. Bobier and M. C. W. Campbell and an NSERC University Research Fellowship to M. C. W. Campbell.

REFERENCES

- H. C. Howland and B. J. Howland, "Photorefractive: a technique for the study of refractive state at a distance," *J. Opt. Soc. Am.* **64**, 240–249 (1974).
- H. C. Howland, O. J. Braddick, J. S. Atkinson, and B. J. Howland, "Optics of photorefractive: orthogonal and isotropic methods," *J. Opt. Soc. Am.* **73**, 1701–1708 (1983).
- J. Atkinson, O. J. Braddick, L. Ayling, E. Pimm-Smith, H. S. Howland, and R. M. Ingram, "Isotropic photorefractive: a new method for refractive testing of infants," in *Pathophysiology of the Visual System*, L. Maffei, ed., Vol. 30 of Documents in Ophthalmological Proceedings Series (Junk, The Hague, 1981), pp. 217–223.
- W. R. Bobier, "Eccentric photorefractive: a method to measure accommodation of highly hypermetropic infants," *Clin. Vision Sci.* **5**, 45–60 (1990).
- W. R. Bobier and O. J. Braddick, "Eccentric photorefractive: optical analysis and empirical measures," *Am. J. Optom. Physiol. Opt.* **62**, 614–620 (1985).
- H. C. Howland, "Optics of photorefractive: results from ray tracing," *Am. J. Optom. Physiol. Opt.* **62**, 621–625 (1985).
- W. R. Bobier, M. C. W. Campbell, C. R. McCreary, A. M. Power, and K. C. Yang, "Coaxial photorefractive methods: an optical analysis," *Appl. Opt.* **31**, 3601–3615 (1992).
- W. R. Bobier, M. C. W. Campbell, C. R. McCreary, A. M. Power, and K. C. Yang, "Geometrical optical analysis of photorefractive methods," *Ophthal. Physiol. Opt.* **12**, 147–152 (1992).
- M. C. W. Campbell, W. R. Bobier, C. R. McCreary, A. M. Power, and K. C. Yang, "The effect of the eye's chromatic aberration on coaxial photorefractive patterns: a geometrical optical analysis," in *Ophthalmic and Visual Optics*, Vol. 3 of 1992 OSA Technical Digest Series (Optical Society of America, Washington, D.C., 1992), pp. 8–11.
- W. N. Charman, "Optics of the human eye," in *Vision and Visual Dysfunction*, J. Cronly-Dillon, ed. (CRC, Boca Raton, Fla., 1991), Vol. 1, W. N. Charman, ed., pp. 1–26.
- F. W. Campbell and R. W. Gubisch, "Optical quality of the human eye," *J. Physiol. (London)* **86**, 558–578 (1966).
- A. G. Bennett and R. B. Rabbetts, *Clinical Visual Optics*, 2nd ed. (Butterworth, London, 1989).
- M. Koomen, R. Tousey, and R. Scolnik, "The spherical aberration of the eye," *J. Am. Optom. Assoc.* **39**, 370–376 (1949).
- A. Ivanoff, "On the influence of accommodation on spherical aberration of the human eye, an attempt to interpret night myopia," *J. Opt. Soc. Am.* **37**, 730–731 (1947).
- M. Koomen, R. Scolnik, and R. Tousey, "A study of night myopia," *J. Opt. Soc. Am.* **41**, 80–90 (1951).
- H. C. Howland and B. Howland, "A subjective method for the measurement of monochromatic aberrations of the eye," *J. Opt. Soc. Am.* **67**, 1508–1518 (1977).
- G. Walsh and W. N. Charman, "Measurement of the axial wavefront aberration of the human eye," *Ophthal. Physiol. Opt.* **5**, 23–31 (1985).
- P. Artal, J. Santamaria, and J. Bescos, "Retrieval of wave aberration of human eyes from actual point-spread-function data," *J. Opt. Soc. Am. A* **5**, 1201–1206 (1988).
- W. R. Bobier, A. Roorda, and M. C. W. Campbell, "Photorefractive equations for chromatic and spherical aberrations," *Invest. Ophthalmol. Vis. Sci.* **33**, 709 (1992).
- I. J. Hodgkinson, K. M. Chong, and A. C. B. Molteno, "Photorefractive of the living eye: a model for linear knife edge photoscreening," *Appl. Opt.* **30**, 2253–2269 (1991).
- A. C. B. Molteno, I. Hoare-Nairne, I. C. Parr, A. Simpson, I. J. Hodgkinson, N. E. O'Brien, and S. D. Watts, "The Otago photoscreener, a method for the mass screening of infants to detect squint and refractive errors," *Trans. Ophthalmol. Soc. N.Z.* **35**, 43–49 (1983).
- F. Berny and S. Slansky, "Wavefront determination resulting from Foucault test as applied to the human eye and visual instruments," in *Optical Instruments and Techniques*, J. Home Dickon, ed. (Oriel, London, 1969), pp. 375–385.
- J. Knight and H. C. Howland, "Off-axis comatic aberrations of the eye (irregular astigmatism) measured by conventional infrared photorefractive," *Invest. Ophthalmol. Vis. Sci.* **30**, 508 (1989).
- A. C. B. Molteno and G. F. Sanderson, "Spherical aberration in human infant eyes," *Trans. Ophthalmol. Soc. N. Z.* **36**, 69–71 (1984).
- W. Wesemann, A. M. Norcia, and D. Allen, "Theory of eccentric photorefractive (photorefractive): astigmatic eyes," *J. Opt. Soc. Am. A* **8**, 2038–2047 (1991).
- R. S. Longhurst, *Geometrical and Physical Optics*, 2nd ed. (Longman, London, 1967).
- M. C. W. Campbell, E. M. Harrison, and P. Simonet, "Psychophysical measurement of the blur on the retina due to optical aberrations of the eye," *Vision Res.* **30**, 1587–1602 (1990).
- M. Millodot and C. Bobier, "The state of accommodation during the measurement of axial chromatic aberration of the eye," *Am. J. Optom. Physiol. Opt.* **53**, 168–172 (1976).
- G. Wald and D. R. Griffin, "The change in refractive power of the human eye in dim and bright light," *J. Opt. Soc. Am.* **37**, 321–336 (1947).
- R. E. Bedford and G. Wysecki, "Axial chromatic aberration of the human eye," *J. Opt. Soc. Am.* **47**, 564–565 (1957).
- J. Atkinson, O. Braddick, K. Durden, P. G. Watson, and S. Atkinson, "Screening for refractive errors in 6–9 month old infants using photorefractive," *Br. J. Ophthalmol.* **68**, 105–112 (1984).
- W. R. Bobier, "Eccentric photorefractive," Ph.D. dissertation (Darwin College, Cambridge, UK, 1987).
- T. C. A. Jenkins, "Aberrations of the eye and their effects on vision. Part I. Spherical aberration," *Br. J. Physiol. Opt.* **20**, 59–91 (1963).
- M. Millodot, "Accommodation and refraction of the eye," in *The Senses*, H. B. Barlow and J. D. Mollon, eds. (Cambridge U. Press, Cambridge, 1982), pp. 62–81.